Bonn-Gatchina analysis of the η photo-production reactions

Andrey Sarantsev

Petersburg Nuclear Physics Institute

HISKP, Uni-Bonn, Germany

NRC Kurchatov Institute, PNPI, Russia

NSTAR2019, Bonn, June 11, 2019

Bonn-Gatchina partial wave analysis group:

A. Anisovich, E. Klempt, V. Nikonov, A. Sarantsev, U. Thoma.

http://pwa.hiskp.uni-bonn.de/

Petersburg Nuclear Physics Institute

Bonn-Gatchina Partial Wave Analysis

Address: Nussallee 14-16, D-53115 Bonn   Fax: (+49) 228 / 73-2505

Data Base | Meson Spectroscopy | Baryon Spectroscopy | NN-interaction | Formalism

Analysis of Other Groups

- SAID
- MAID
- Giessen Uni

BG PWA

- Publications
- Talks
- Contacts

Useful Links

- SPIRES
- PDG Homepage
- Durham Data Base
- Bonn Homepage

CB-ELSA Homepage

Responsible: Dr. V. Nikonov, E-mail: *nikonov@hiskp.uni-bonn.de*
Last changes: January 26th, 2010.

Recently included meson photoproduction data

DATA	2011-2016	added in 2016-2018
$\gamma n \to \Lambda K, \Sigma^- K$		$\frac{d\sigma}{d\Omega}$ **(CLAS), E (CLAS)**
$\gamma n \to \pi^- p$	$\frac{d\sigma}{d\Omega}, \Sigma, P$	E, Σ **(CLAS)**
$\gamma n \to \eta n$ $\gamma p \to \eta p$ $\gamma p \to \eta' p$	$\frac{d\sigma}{d\Omega}, \Sigma$ $\frac{d\sigma}{d\Omega}, \Sigma(GRAAL)$	$\frac{d\sigma}{d\Omega}$ **(MAMI)** $\frac{d\sigma}{d\Omega}(h = \frac{1}{2})$ **(CB-ELSA)** $\frac{d\sigma}{d\Omega}, F, T$ **(MAMI)** T, P, H, G**,(CB-ELSA)** E, Σ **(CB-ELSA,CLAS)** $\frac{d\sigma}{d\Omega}, \Sigma$
$\gamma p \to K^+ \Lambda$ $\gamma p \to K^+ \Sigma^0$	$\frac{d\sigma}{d\Omega}, \Sigma, P, T, C_x, C_z, O_{x'}, O_{z'}$ $\frac{d\sigma}{d\Omega}, \Sigma, P, C_x, C_z$	Σ, P, T, O_x, O_z **(CLAS)** Σ, P, T, O_x, O_z **(CLAS)**
$\pi^- p \to \pi^+ \pi^- n$ $\pi^- p \to \pi^- \pi^0 p$		$d\sigma/d\Omega$ **(HADES)** $d\sigma/d\Omega$ **(HADES)**
$\gamma p \to \pi^0 \pi^0 p$ $\gamma p \to \pi^+ \pi^- p$	$d\sigma/d\Omega, \Sigma, E, I_c, I_s$	T, P, H, F, P_x, P_y **(CB-ELSA)** $d\sigma/d\Omega, I_c, I_s$ **(CLAS)**
$\gamma p \to \omega p$	$d\sigma/d\Omega, \Sigma, \rho^k_{ij}, E, G$ **(CB-ELSA)**	Σ **(CLAS) P,T,F,H (CLAS)**
$\gamma p \to K^* \Lambda$		$d\sigma/d\Omega$**,** ρ_{ij}

The analysis of the new $\gamma p \to \eta p$ data.

New MAMI data: a strong cusp effect from the $\eta' p$ channel

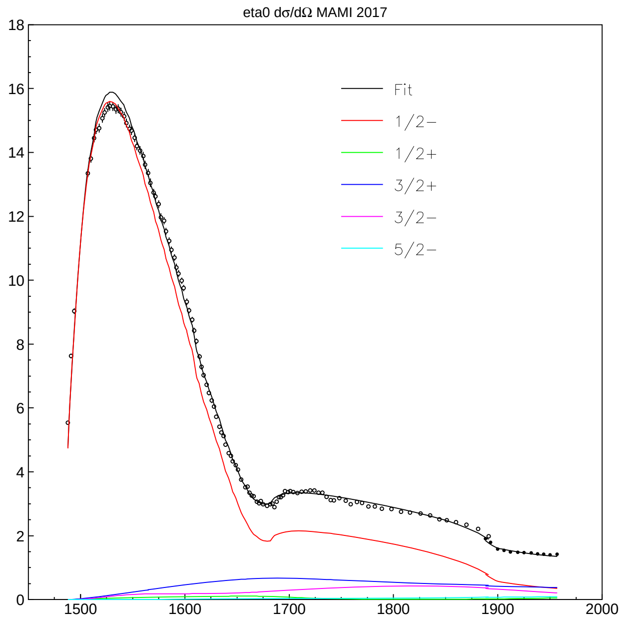

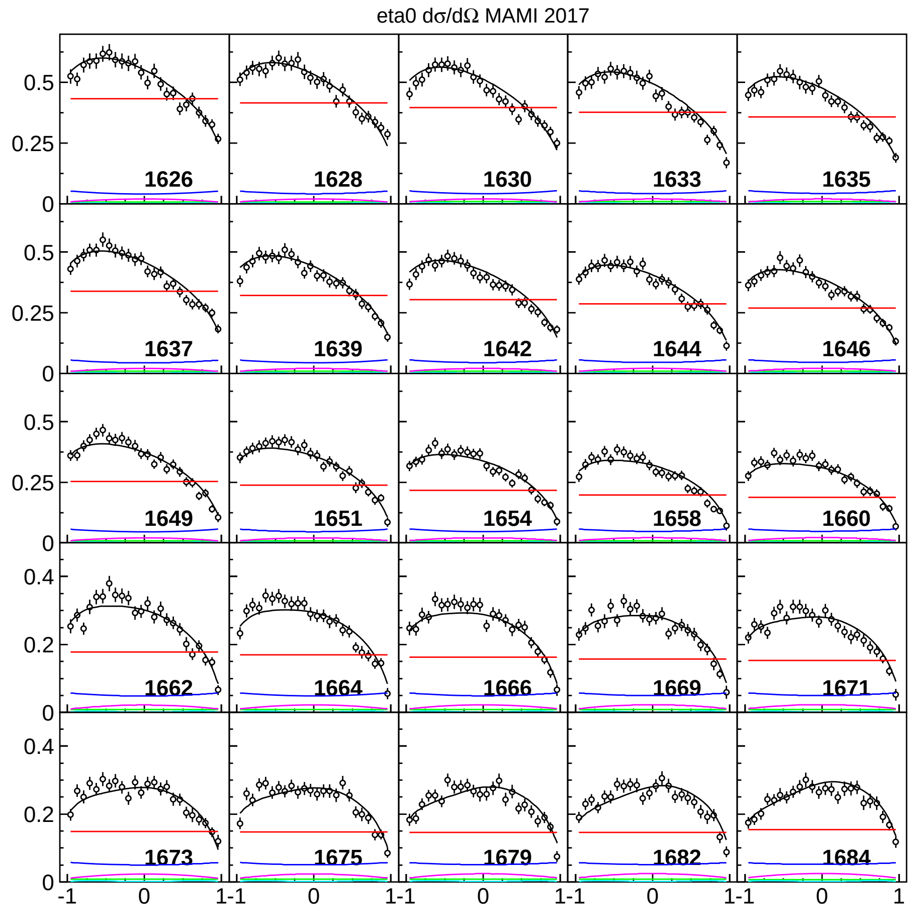

N/D based (D-matrix) analysis of the data

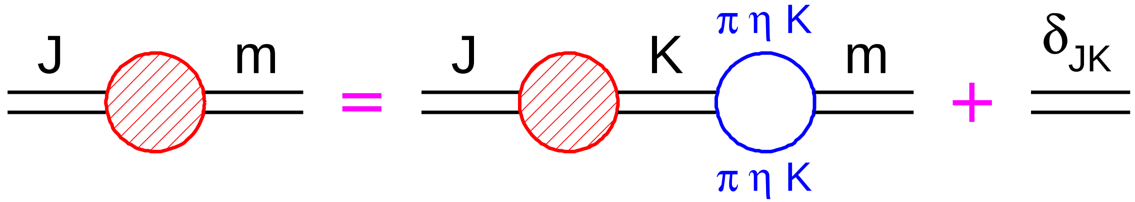

$$D_{jm} = D_{jk} \sum_{\alpha} B_{\alpha}^{km}(s) \frac{1}{M_m - s} + \frac{\delta_{jm}}{M_j^2 - s} \qquad \hat{D} = \hat{\kappa}(I - \hat{B}\hat{\kappa})^{-1}$$

$$\hat{\kappa} = diag\left(\frac{1}{M_1^2 - s}, \frac{1}{M_2^2 - s}, \ldots, \frac{1}{M_N^2 - s}, R_1, R_2 \ldots \right)$$

$$\hat{B}_{ij} = \sum_{\alpha} B_{\alpha}^{ij} = \sum_{\alpha} \int \frac{ds'}{\pi} \frac{g_{\alpha}^{(R)i} \rho_{\alpha}(s', m_{1\alpha}, m_{2\alpha}) g_{\alpha}^{(L)j}}{s' - s - i0}$$

In the present fits we calculate the elements of the B^{ij}_α using one subtraction taken at the channel threshold $M_\alpha = (m_{1\alpha} + m_{2\alpha})$:

$$B^{ij}_\alpha(s) = B^{ij}_\alpha(M^2_\alpha) + (s - M^2_\alpha) \int\limits_{M^2_a}^{\infty} \frac{ds'}{\pi} \frac{g^{(R)i}_\alpha \rho_\alpha(s', m_{1\alpha}, m_{2\alpha}) g^{(L)j}_\alpha}{(s' - s - i0)(s' - M^2_\alpha)} .$$

In this case the expression for elements of the $\hat{B}$ matrix can be rewritten as:

$$B^{ij}_\alpha(s) = g^{(R)i}_a \left(b^\alpha + (s - M^2_\alpha) \int\limits_{M^2_a}^{\infty} \frac{ds'}{\pi} \frac{\rho_\alpha(s', m_{1\alpha}, m_{2\alpha})}{(s' - s - i0)(s' - M^2_\alpha)} \right) g^{(L)j}_\beta = g^{(R)i}_a B_\alpha g^{(L)j}_\beta$$

and D-matrix method equivalent to the K-matrix method with loop diagram with real part taken into account:

$$A = \hat{K}(I - \hat{B}\hat{K})^{-1} \qquad\qquad B_{\alpha\beta} = \delta_{\alpha\beta} B_\alpha$$

The analysis of the new $\gamma p \to \eta p$ data. $d\sigma/d\Omega$ (MAMI)

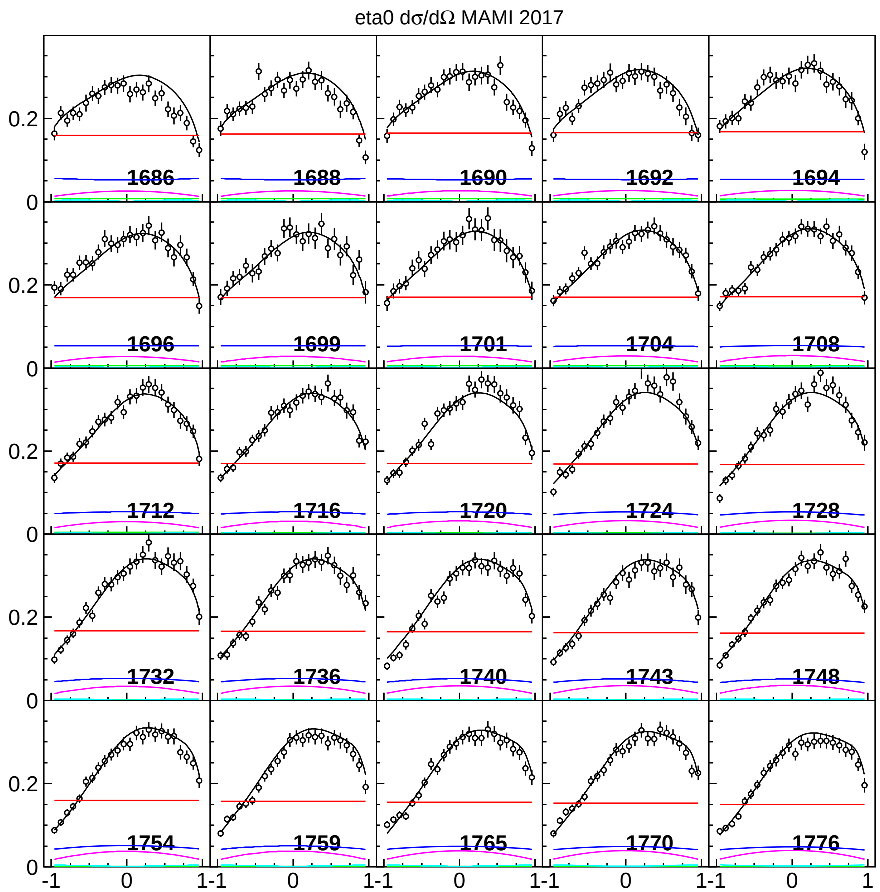

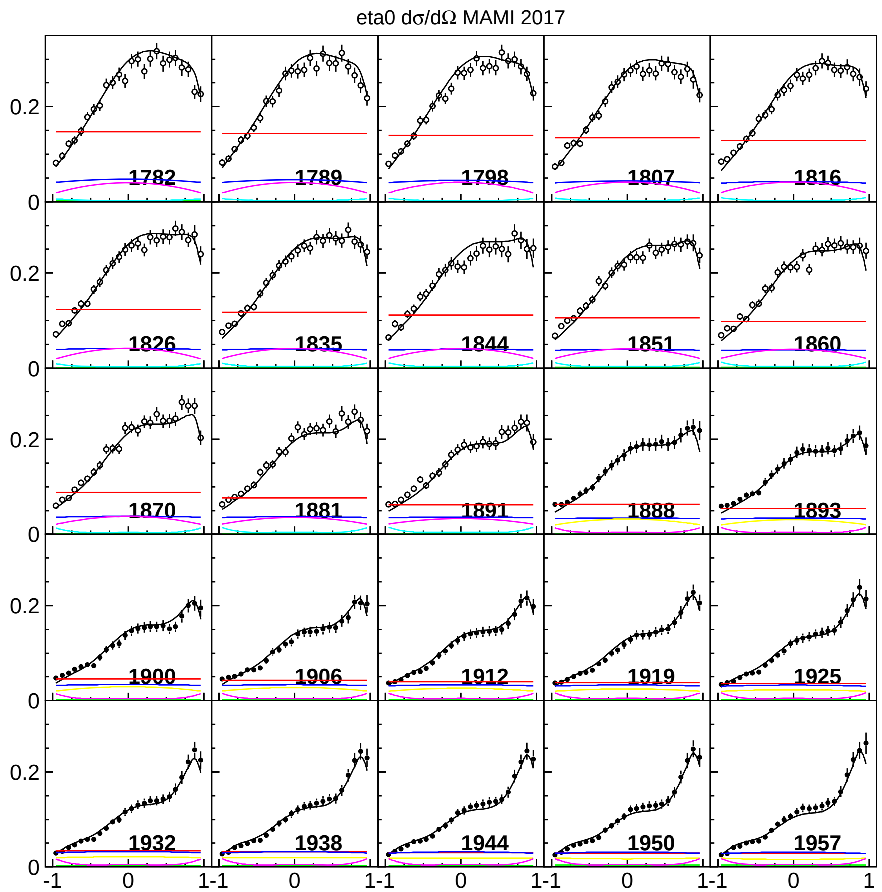

The analysis of the new $\gamma p \to \eta p$ data. H, P, T (CB-ELSA, Preliminary)

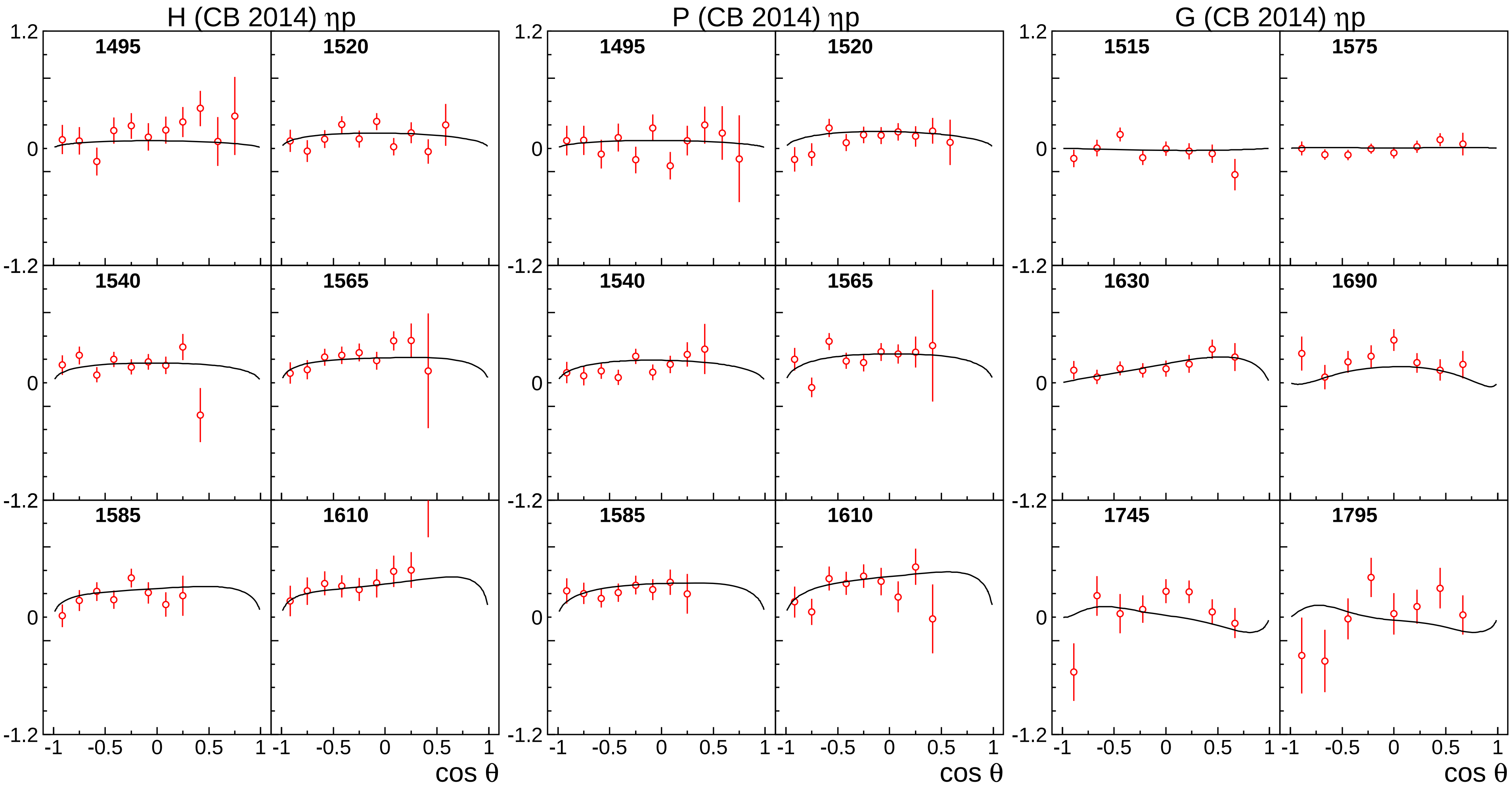

The analysis of the new $\gamma p \to \eta p$ data. T (CB-ELSA, Preliminary), (MAMI scale 1.4)

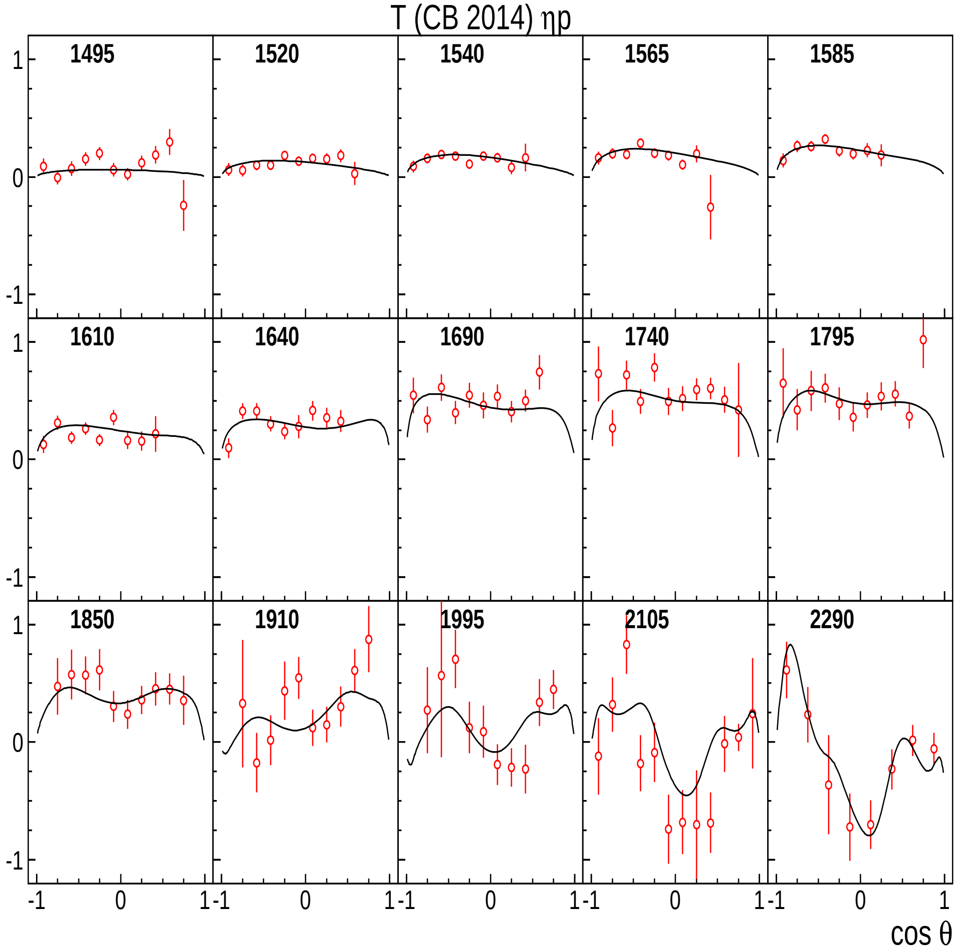

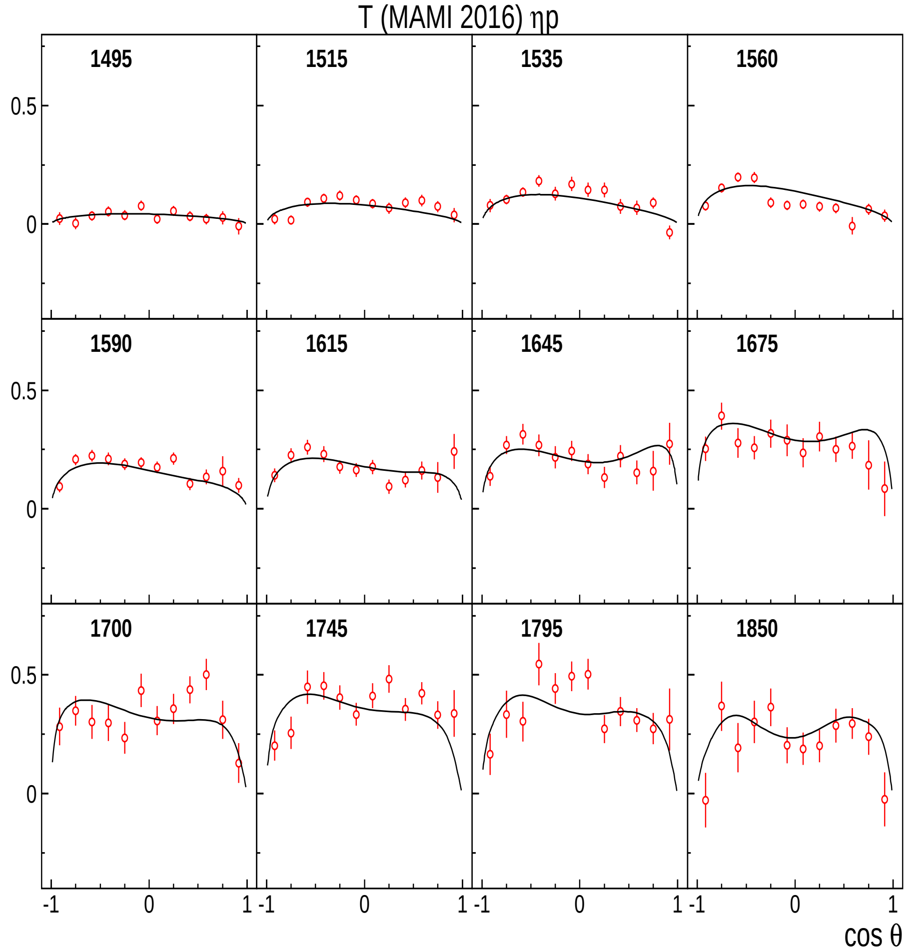

The analysis of the new $\gamma p \to \eta p$ data. E (CB-ELSA, Preliminary), F (MAMI) (scale 1.4)

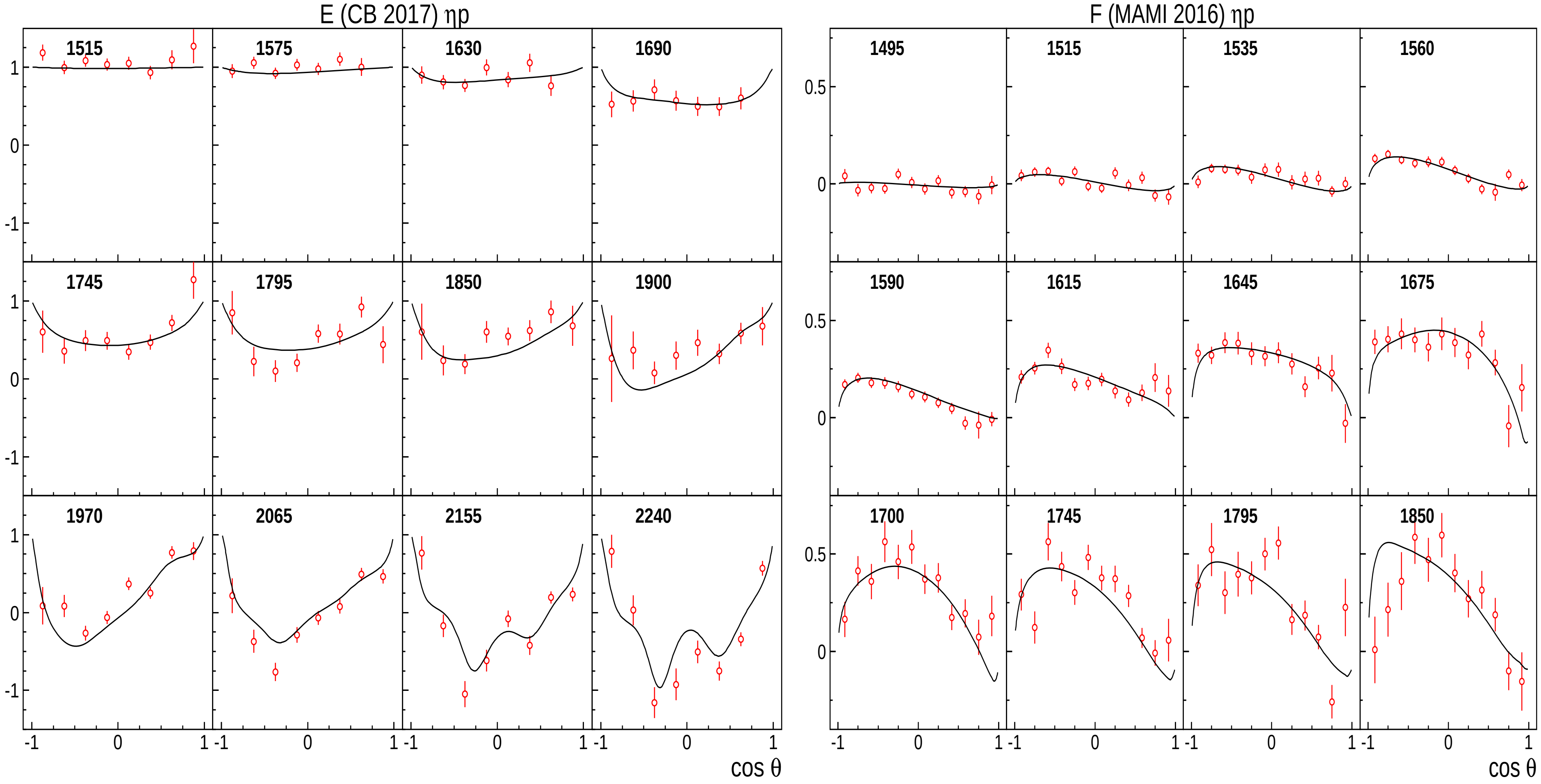

The analysis of the new $\gamma p \to \eta p$ data. Σ (CB-ELSA and CLAS)

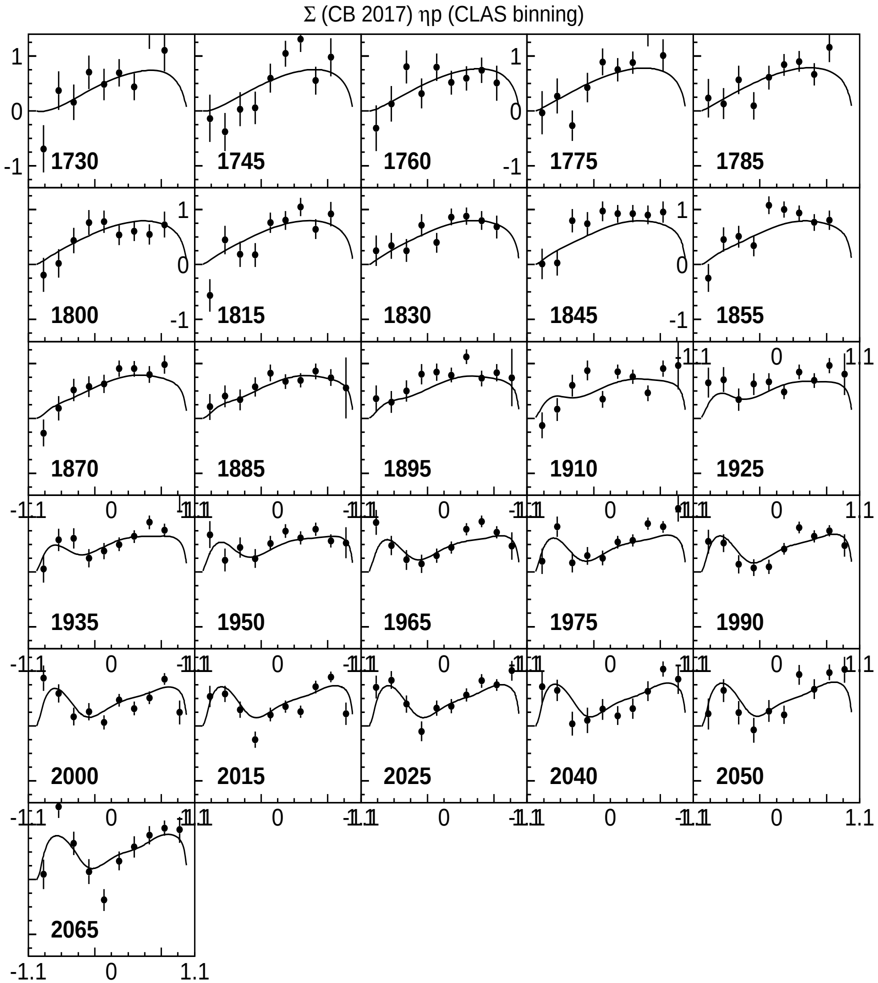

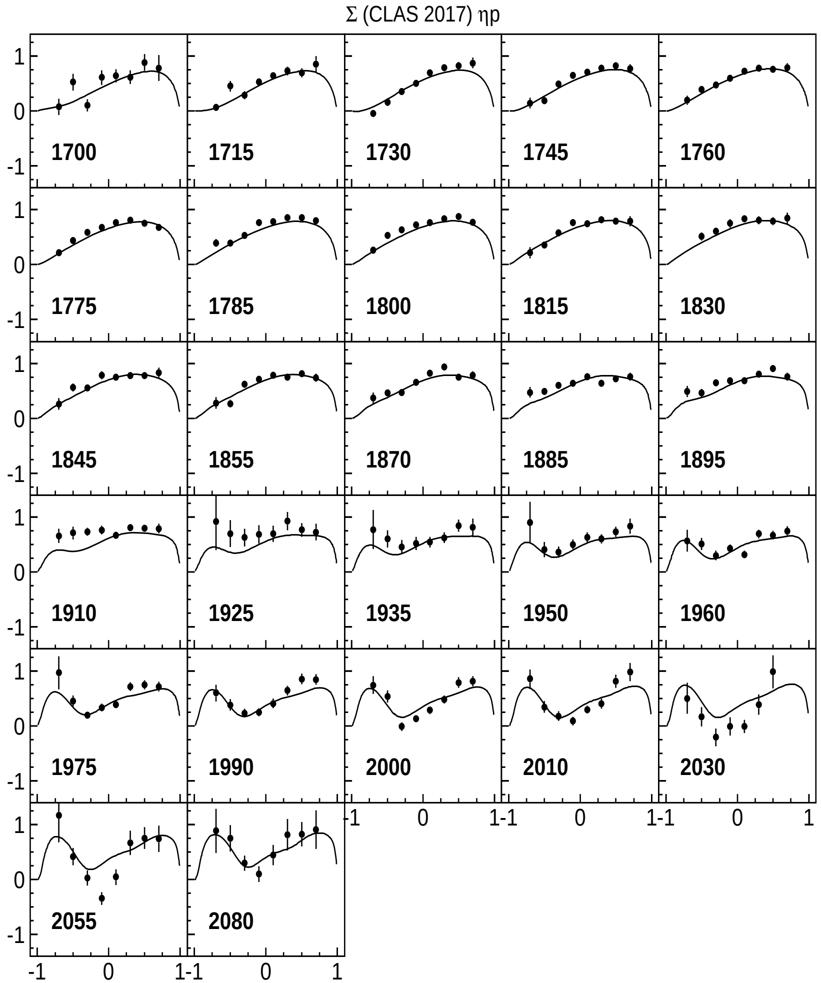

The analysis of the $\gamma p \to \eta' p$ data.

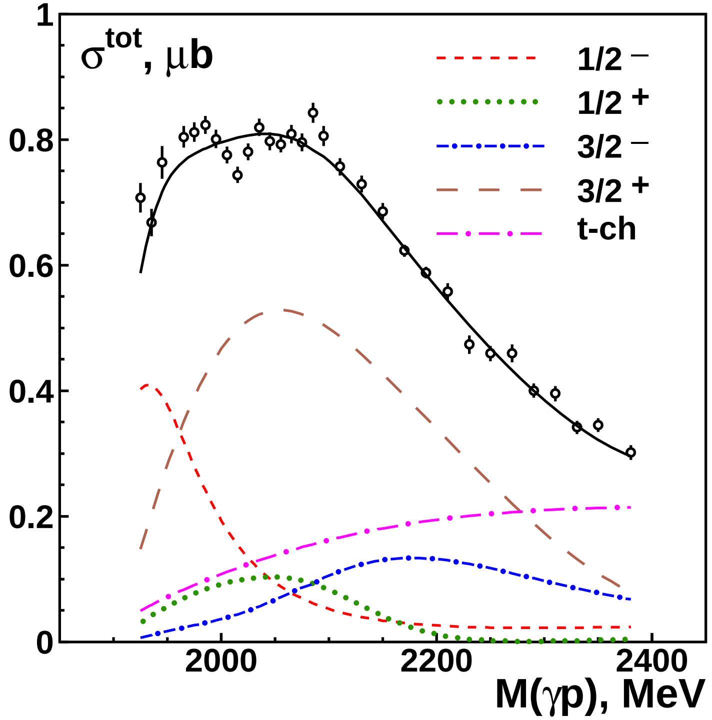

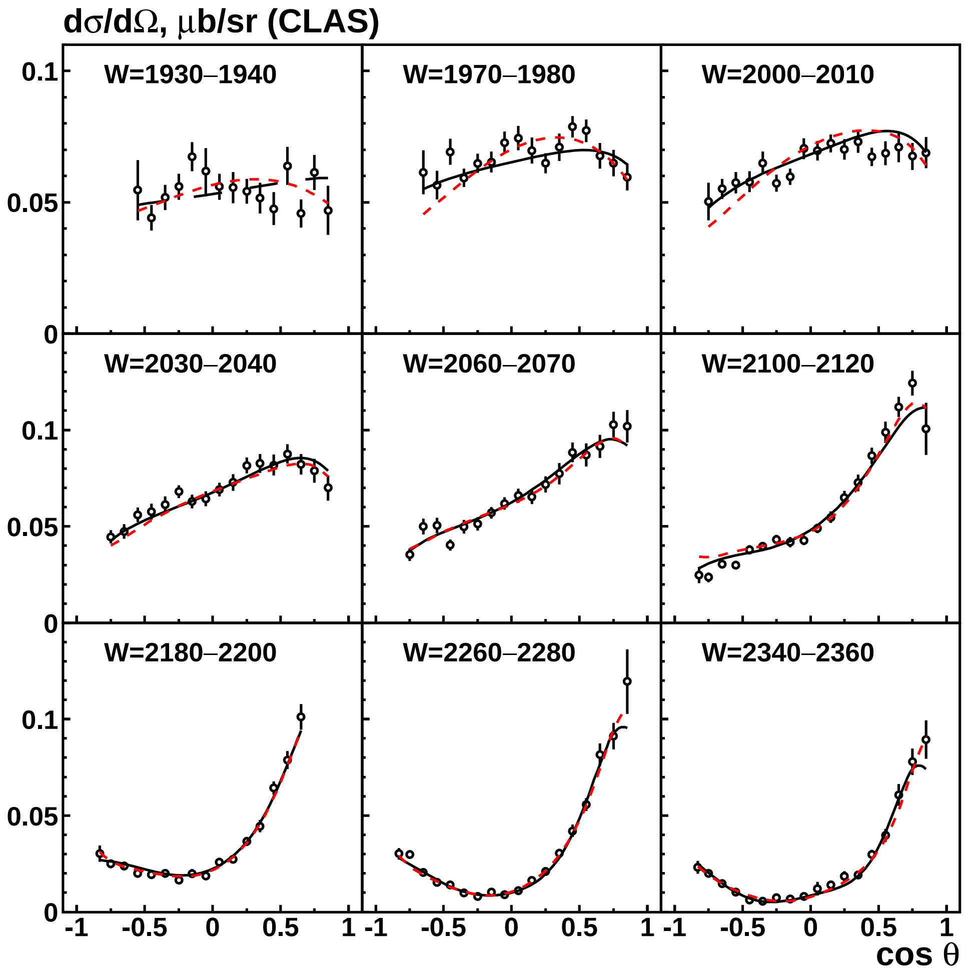

Strong contribution from the $S_{11}(1895)$, $P_{13}(1900)$, $P_{11}(2100)$ and $D_{13}(2120)$ states.

MAMI differential cross section

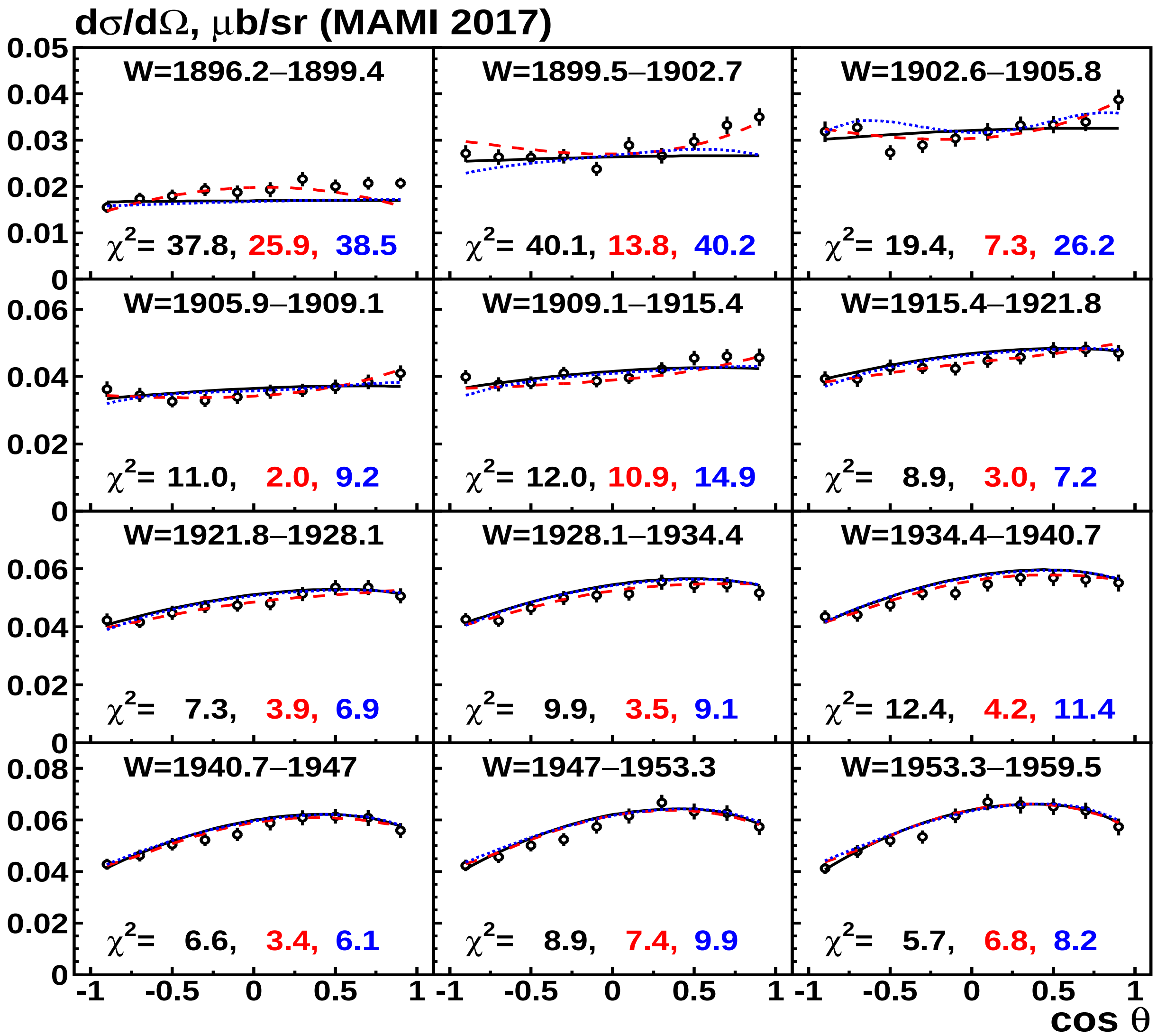

The beam asymmetry on $\gamma p \to \eta' p$

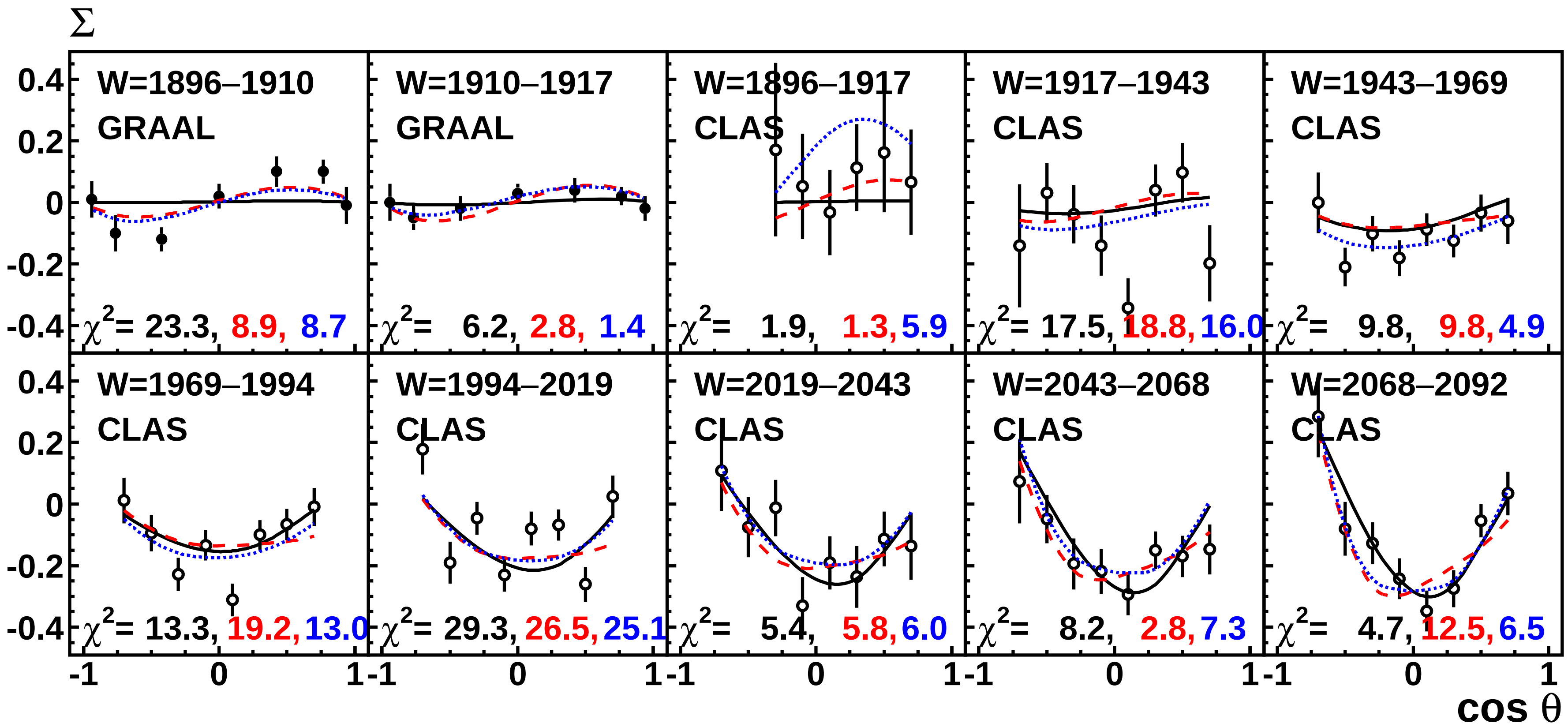

No narrow states $D_{15}(1903)$ $D_{13}(1900)$

$$BR = \int_{\text{threshold}}^{\infty} \frac{ds}{\pi} \frac{(g_a^\alpha)^2 \rho_a^\alpha(s)}{(M_{\text{BW}}^{\alpha\ 2} - s)^2 + (\sum_\alpha g_a^{\alpha\ 2} \rho_a^\alpha(s))^2}$$

Table 1: The masses and widths M_{pole},Γ_{pole} are given in MeV, the moduli of the helicity couplings in 10^{-3} GeV$^{-1/2}$. $\Delta\pi$ denotes $\Delta(1232)3/2^+\pi$ and $N^*\pi$, $N(1520)3/2^-\pi$.

	M_{pole}	Γ_{pole}	Branching ratios (in %) for $N^* \rightarrow$						
			$N\eta'$	$N\pi$	$N\eta$	$N\omega$	$\Delta\pi$	$N^*\pi$	$N\sigma$
$N(1895)1/2^-$	**1907$\pm$10**	100^{+40}_{-10}	**13$\pm$5**	**2.5$\pm$1.5**	**10$\pm$5**	**28$\pm$12**	**7$\pm$4**	**-**	**-**
$N(2100)1/2^+$	**2100$\pm$30**	**280$\pm$35**	**8$\pm$3**	**13$\pm$5**	**25$\pm$10**	**15$\pm$10**	**10$\pm$4**	**30$\pm$4**	**20$\pm$6**
$N(2120)3/2^-$	**2115$\pm$40**	**345$\pm$35**	**4$\pm$2**	**5$\pm$3**	**3$\pm$2**	**12$\pm$8**	**70$\pm$23**		**11$\pm$4**
$N(1900)3/2^+$	**1910$\pm$30**	**280$\pm$50**	**6$\pm$2**	**3$\pm$2**	**3$\pm$1**	**15$\pm$9**	**50$\pm$15**	**15$\pm$8**	**4$\pm$3**

The description of the data below W=1917 MeV and the prediction of other observables

Resonance	N	Basic	D_{13}	D_{15}
M (MeV)			1900	1903
Γ (MeV)			1	1
χ^2 (Σ)	13	29.5	11.7	10.1
χ^2 $(\frac{d\sigma}{d\Omega})$	50	120.3	59.9	129.0

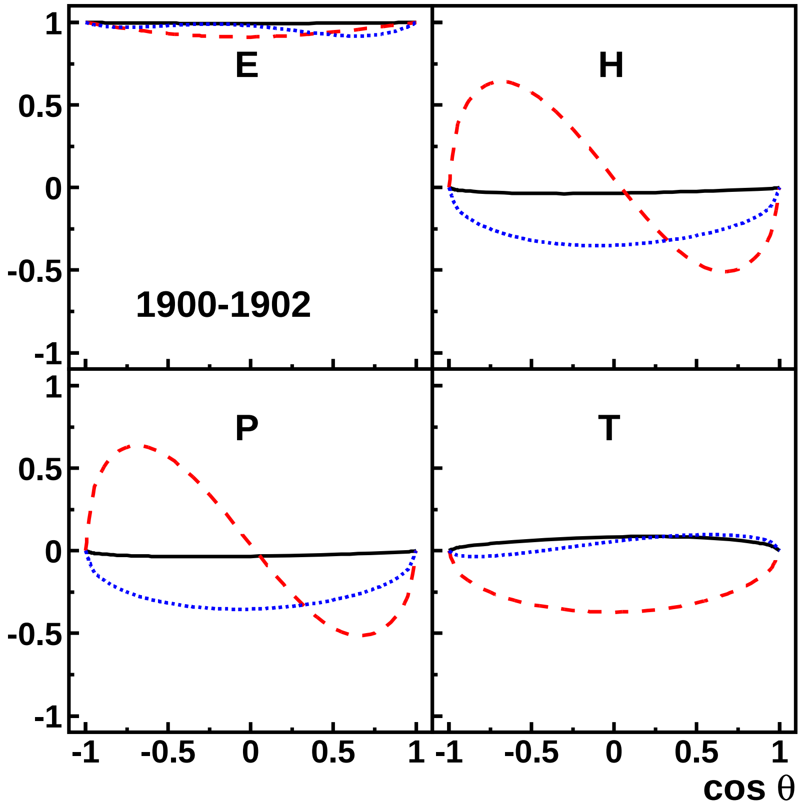

The description of the $\gamma n \to \eta n$ data with N/D-based approach

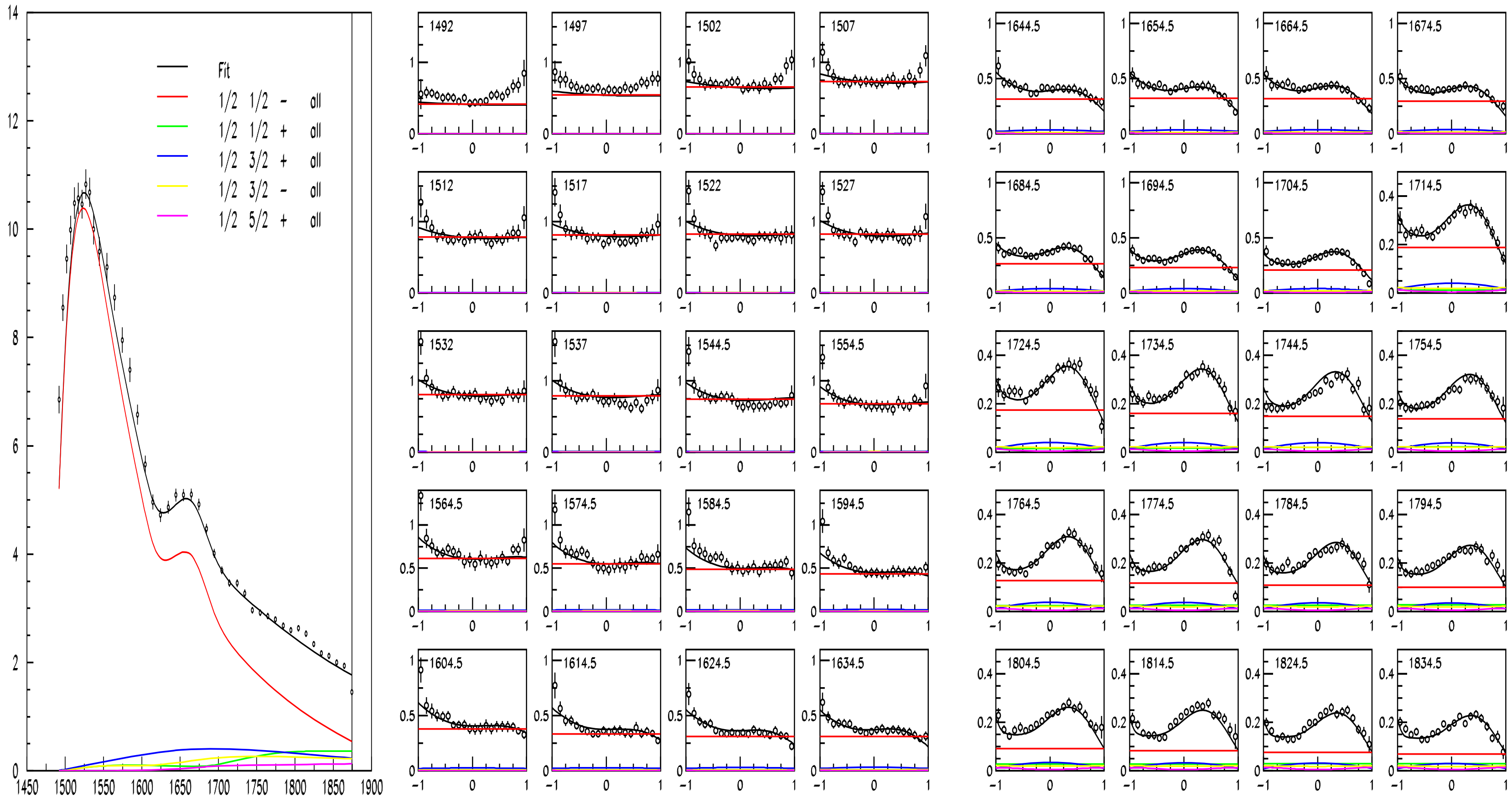

The description of the differential cross section and beam asymmetry in the selected energy region

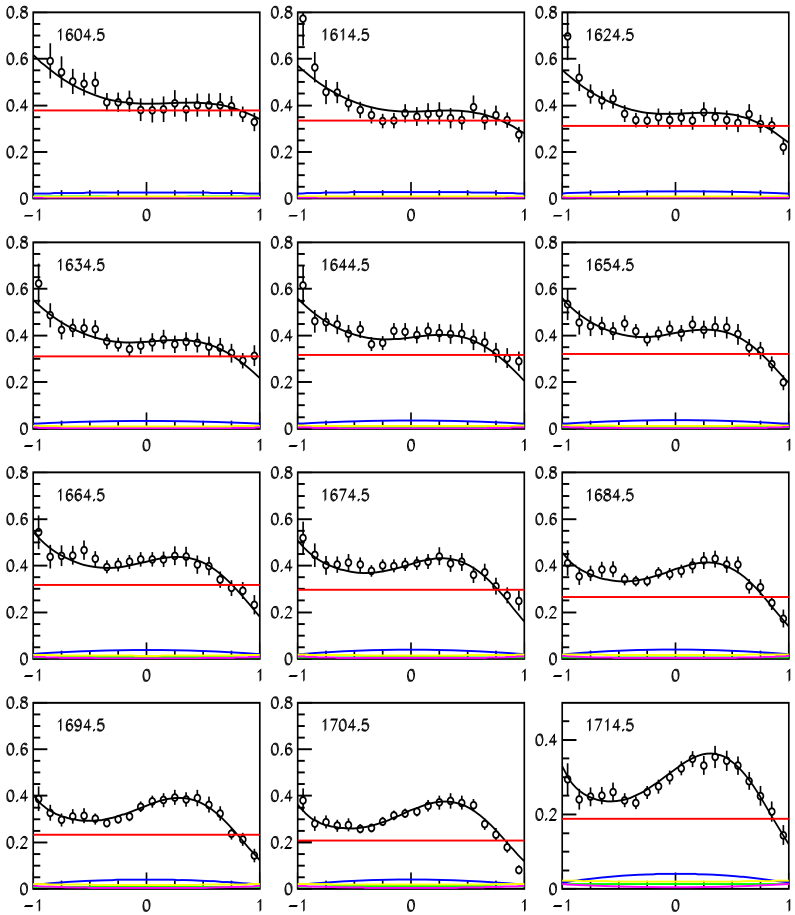

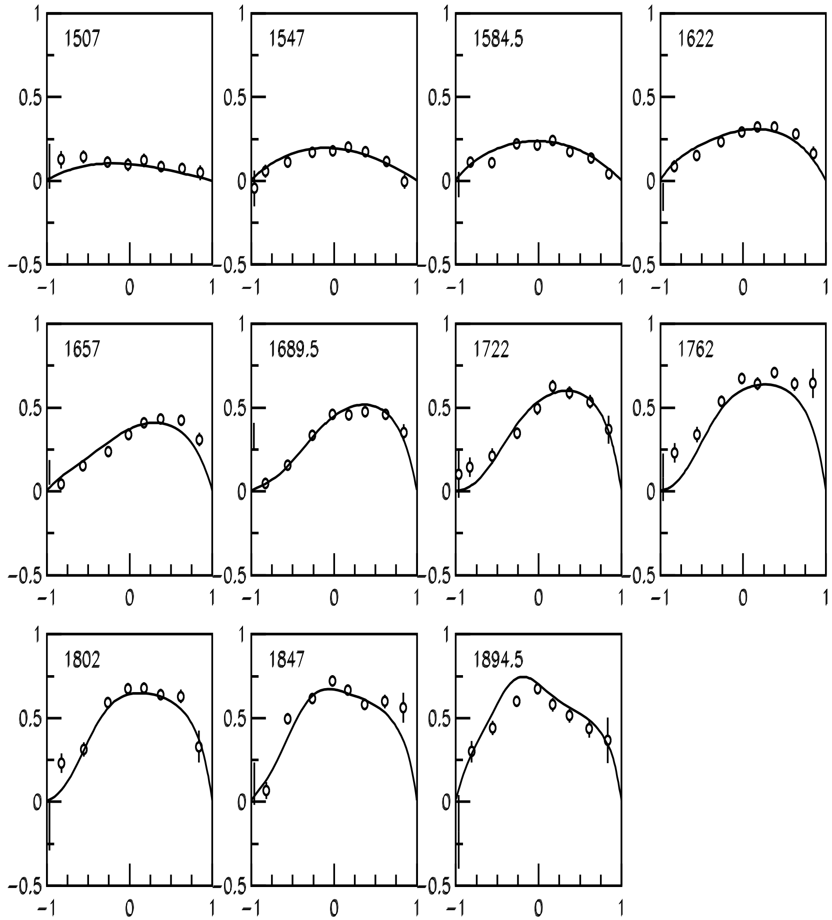

The description of the $\pi p \to \eta p$ data with N/D-based approach

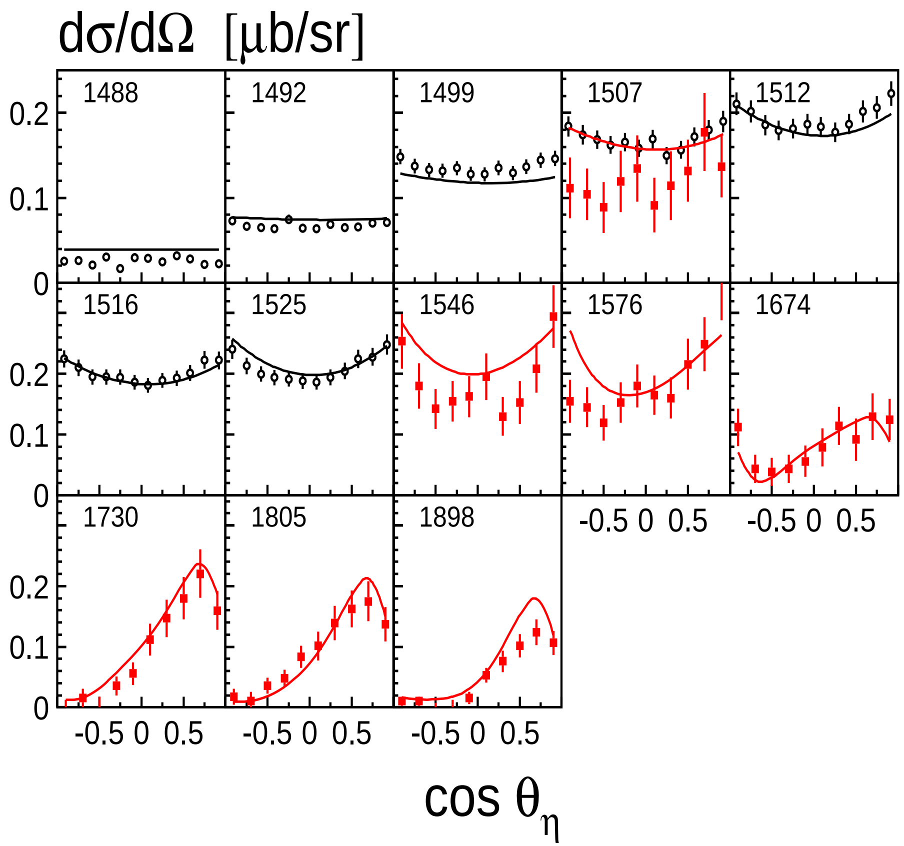

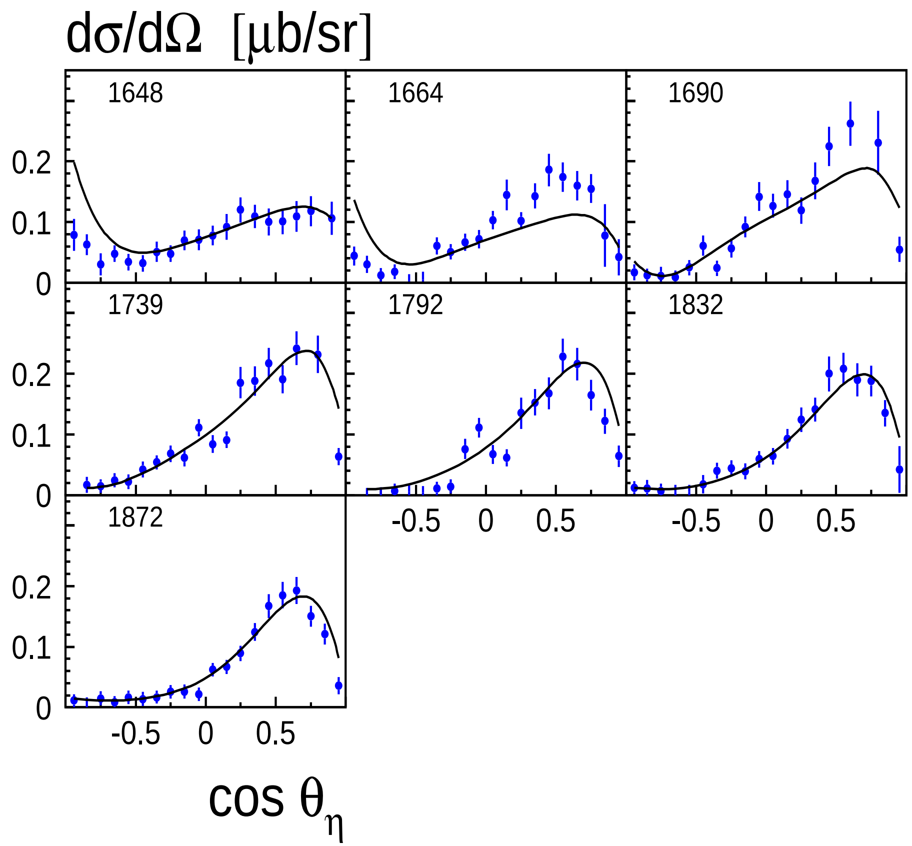

S. Prakhov et al., Phys. Rev. C72(2005) 015203

R.M. Brown et al. Nucl. Phys. B153, 89 (1979)

W. B. Richards et al., Phys. Rev. D1, 10 (1970)

Residues in the pole for $\pi N \to \eta N$ (MeV) and $\gamma N \to \eta N$ (10^{-3} GeV$^{-\frac{1}{2}}$) reactions amplitudes.

Res	$N(1535)1/2^-$		$N(1650)1/2^-$		$N(1895)1/2^-$	
$\pi N \to \eta N$	**(29±2)**	**-(84±3)^o**	**-(22±3)**	**(2±12)^o**	**(5±3)**	**(25±20)^o**
$\gamma p \to \eta p$ **(E,-$A^{\frac{1}{2}}$)**	**-(19±2)**	**-(60±3)^0**	**(4±0.3)**	**(31±10)^o**	**(1.7±0.8)**	**(20±20)^o**
Res	$N(1440)1/2^+$		$N(1710)1/2^+$		$N(1880)1/2^+$	
$\pi N \to \eta N$	**-(20±6)**	**(0±30)^o**	**(7±2)**	**(54±15)^o**	**(12±5)**	**(60±18)^o**
$\gamma p \to \eta p$ **(M,$A^{\frac{1}{2}}$)**	**(5±2)**	**(15±30)^o**	**(2.2±0.7)**	**-(73±16)^o**	**(0.9±0.35)**	**(60±17)^o**
Res	$N(1520)3/2^-$		$N(1720)3/2^+$		$N(1900)3/2^+$	
$\pi N \to \eta N$	**(1.7±0.4)**	**-(88±15)^o**	**(8.1±2.6)**	**(45±10)^o**	**(2.9±0.8)**	**(55±30)^o**
$\gamma p \to \eta p$ ($A^{\frac{1}{2}}$)	**(0.22±0.06)**	**(86±18)^o**	**(8.7±3.0)**	**(49±10)^o**	**-(1.3±0.4)**	**-(40±25)^o**
$\gamma p \to \eta p$ ($A^{\frac{3}{2}}$)	**(1.18±0.20)**	**-(74±17)^o**	**-(4.0±2.1)**	**-(53±12)^o**	**(12±5)**	**(14±10)^o**
$\gamma p \to \eta p$ **(E)**	**-(0.91±0.15)**	**-(71±16)^0**	**-(4.3±1.7)**	**(35±15)^o**	**(4.0±1.3)**	**(6±12)^o**
$\gamma p \to \eta p$ **(M)**	**-(0.44±0.10)**	**-(79±14)^0**	**-(6.1±2.7)**	**-(98±14)^o**	**-(10.0±4)**	**(17±12)^o**

Conclusion

1. **The drop of the $\gamma p \to \eta p$ total cross section in the mass region around 1900 MeV together with a strong increase of the $\eta - prime$ cross section can be explained naturally with the existence of the $N(1895)1/2^-$ state.**

2. **The combined analysis allows us to define the parameters of the $N(1895)1/2^-$ state with a good precision.**

3. **The obtained description of the η photoproduction data allows us to describe the $\gamma n \to \eta n$ data by fitting only the γn helicity couplings.**

4. **The beam asymmetry GRAAL data and the MAMI differential cross section on the $\eta - prime$ photoproduction show an anomaly near $\eta' p$ threshold. This anomaly can be explained with a presence of a very narrow state. However the data should be carefully checked and measurements of other polarization observables are greatly welcome.**

$\gamma p \rightarrow \eta p$ multipoles

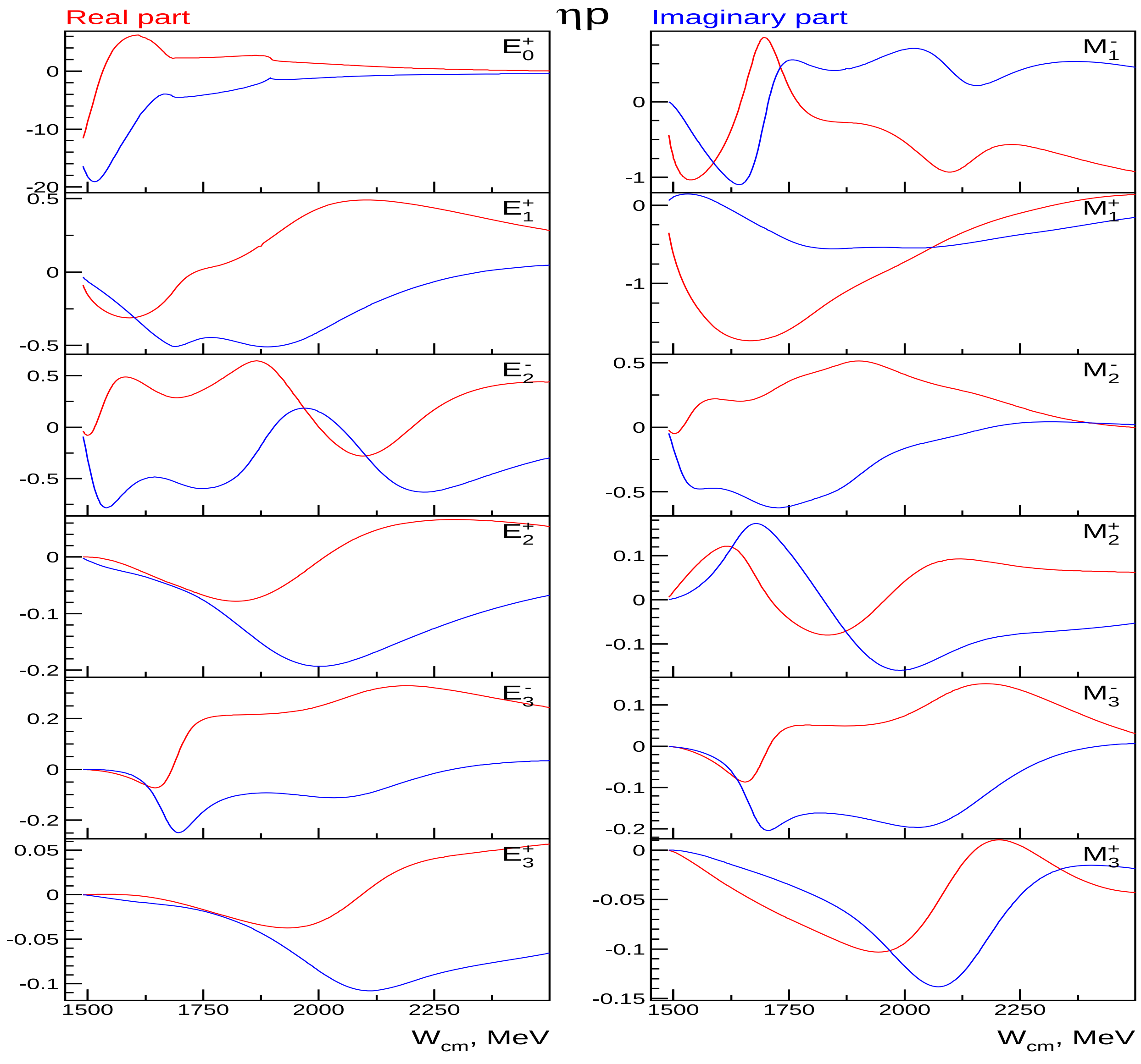

Amplitudes squared for the $\pi N \to \eta N$ and $\gamma p \to \eta p$ reactions